

Altered carnitine homeostasis is associated with decreased mitochondrial function and altered nitric oxide signaling in lambs with pulmonary hypertension

Shruti Sharma,¹ Neetu Sud,¹ Dean A. Wiseman,¹ A. Lee Carter,² Sanjiv Kumar,¹ Yali Hou,¹ Thomas Rau,³ Jason Wilham,³ Cynthia Harmon,⁴ Peter Oishi,⁴ Jeffrey R. Fineman,^{4,5} and Stephen M. Black¹

¹Program in Pulmonary Vascular Disease, Vascular Biology Center, and ²Department of Biochemistry and Molecular Biology, Medical College of Georgia, Augusta, Georgia; ³Department of Biomedical and Pharmaceutical Sciences, The University of Montana, Missoula, Montana; and ⁴Department of Pediatrics and ⁵Cardiovascular Research Institute, University of California, San Francisco, California

Submitted 28 June 2007; accepted in final form 13 November 2007

Sharma S, Sud N, Wiseman DA, Carter AL, Kumar S, Hou Y, Rau T, Wilham J, Harmon C, Oishi P, Fineman JR, Black SM. Altered carnitine homeostasis is associated with decreased mitochondrial function and altered nitric oxide signaling in lambs with pulmonary hypertension. *Am J Physiol Lung Cell Mol Physiol* 294: L46–L56, 2008. First published November 16, 2007; doi:10.1152/ajplung.00247.2007.—Utilizing aortopulmonary vascular graft placement in the fetal lamb, we have developed a model (shunt) of pulmonary hypertension that mimics congenital heart disease with increased pulmonary blood flow. Our previous studies have identified a progressive development of endothelial dysfunction in shunt lambs that is dependent, at least in part, on decreased nitric oxide (NO) signaling. The purpose of this study was to evaluate the possible role of a disruption in carnitine metabolism in shunt lambs and to determine the effect on NO signaling. Our data indicate that at 2 wk of age, shunt lambs have significantly reduced expression ($P < 0.05$) of the key enzymes in carnitine metabolism: carnitine palmitoyltransferases 1 and 2 as well as carnitine acetyltransferase (CrAT). In addition, we found that CrAT activity was inhibited due to increased nitration. Furthermore, free carnitine levels were significantly decreased whereas acylcarnitine levels were significantly higher in shunt lambs ($P < 0.05$). We also found that alterations in carnitine metabolism resulted in mitochondrial dysfunction, since shunt lambs had significantly decreased pyruvate, increased lactate, and a reduced pyruvate/lactate ratio. In pulmonary arterial endothelial cells cultured from juvenile lambs, we found that mild uncoupling of the mitochondria led to a decrease in cellular ATP levels and a reduction in both endothelial NO synthase-heat shock protein 90 (eNOS-HSP90) interactions and NO signaling. Similarly, in shunt lambs we found a loss of eNOS-HSP90 interactions that correlated with a progressive decrease in NO signaling. Our data suggest that mitochondrial dysfunction may play a role in the development of endothelial dysfunction and pulmonary hypertension and increased pulmonary blood flow.

carnitine metabolism; oxidative stress

THE DEVELOPMENT OF PULMONARY HYPERTENSION and its associated increased vascular reactivity are common accompaniments of congenital heart disease with increased pulmonary blood flow (3). Endothelial dysfunction is thought to be an early hallmark of pulmonary hypertension (4). There is

increasing histological and physiological evidence that endothelial injury and the resulting aberration in the balance of its regulatory mechanisms play an important role in the development of pulmonary hypertension (4). Children with pulmonary hypertension have evidence of endothelial dysfunction as indicated by impaired endothelium-dependent relaxation in early disease and decreased endothelial nitric oxide synthase (eNOS) protein levels in late disease (11, 23). However, data delineating the role of endothelium-derived NO in the disease have been less clear. For example, we (5) and others (72) have shown that pulmonary expression of NOS can be paradoxically increased during the development of pulmonary hypertension. However, it also has been reported that pulmonary NO production can be decreased when eNOS expression is elevated (1, 56). Therefore, the lack of correlation between elevated eNOS expression and elevated NO activity suggests the presence of other regulatory elements that may be important in the development of pulmonary hypertension.

Disruption of mitochondrial function is acknowledged as a critical event in a number of pathological conditions, including hypoxia-ischemic injuries (6), stroke (59), and diabetes (16, 45, 47, 50). The carnitine acyltransferase pathway has recently been shown to be of critical importance for maintaining normal mitochondrial function. This pathway consists of the carnitine palmitoyltransferases (CPT1 and CPT2) and carnitine acetyltransferase (CrAT), where CPTs transesterify medium- and long-chain fatty acyl chains and CrAT transesterifies short-chain acyl chains. Derangements in these pathways have previously been known to underlie fatty acid oxidation disorders (25, 34, 60, 65). The principal enzyme affected is thought to be CrAT, which catalyzes a reversible reaction between short-chain acyl-CoA and CoA, and acylcarnitine and carnitine. However, the contribution of these integral mitochondrial processes to the pathophysiology of pulmonary hypertension has not been actively investigated. Thus the purpose of this study was to determine whether the abnormalities in flow and pressure in lambs with pulmonary hypertension disrupt lung mitochondrial function and whether this plays a role in disrupting NO signaling.

Address for reprint requests and other correspondence: S. M. Black, Vascular Biology Center, 1459 Laney Walker Blvd., CB3210B, Medical College of Georgia, Augusta, GA 30912 (e-mail: sblack@mcg.edu).

The costs of publication of this article were defrayed in part by the payment of page charges. The article must therefore be hereby marked “advertisement” in accordance with 18 U.S.C. Section 1734 solely to indicate this fact.

Using a lamb model that mimics a congenital heart defect with increased pulmonary blood flow due to the in utero placement of an aorta-to-pulmonary artery vascular graft (53), we identified alterations in carnitine metabolism secondary to a nitration-mediated decrease in CrAT activity. The decrease in CrAT abundance and activity was associated with mitochondrial dysfunction. Furthermore, lamb pulmonary artery endothelial cells with disrupted mitochondrial activity were observed to have a decrease in NO signaling through a reduction in cellular ATP levels and heat shock protein 90 (HSP90) activity. Together, our data support the conclusion that mitochondrial dysfunction secondary to a disruption of carnitine homeostasis may play a role in the progressive loss of NO signaling and the development of endothelial dysfunction and pulmonary hypertension with increased pulmonary blood flow.

MATERIALS AND METHODS

Surgical preparations and care. Twelve mixed-breed Western pregnant ewes (137–141 days of gestation, term = 145 days) were operated on under sterile conditions with the use of local anesthesia (2% lidocaine hydrochloride) and inhalational anesthesia (1–3% isoflurane). A midline incision was made in the ventral abdomen, and the pregnant horn of the uterus was exposed. Through a small uterine incision, the left fetal forelimb and chest were exposed, and a left lateral thoracotomy was performed in the third intercostal space. Additional fetal anesthesia consisted of local anesthesia with 1% lidocaine hydrochloride and ketamine hydrochloride (5 mg im). With the use of side-biting vascular clamps, an 8.0-mm Gore-Tex vascular graft (~2 mm long; W.L. Gore and Associates, Milpitas, CA) was sutured between the ascending aorta and main pulmonary artery with 7.0 proline (Ethicon, Somerville, NJ), using a continuous suture technique. The thoracotomy incision was then closed in layers. This procedure was previously described in detail (53).

Two or four weeks after spontaneous delivery, these lambs and 12 age-matched control lambs were fasted for 24 h with free access to water. The lambs were then anesthetized with ketamine hydrochloride (15 mg/kg im). Under additional local anesthesia with 1% lidocaine hydrochloride, polyurethane catheters were placed in an artery and vein of a hind leg. These catheters were advanced to the descending aorta and the inferior vena cava, respectively. The lambs were then anesthetized with ketamine hydrochloride (~0.3 mg·kg⁻¹·min⁻¹), diazepam (0.002 mg·kg⁻¹·min⁻¹), and fentanyl citrate (1.0 µg·kg⁻¹·h⁻¹), intubated with a 7.0-mm outer diameter (OD) cuffed endotracheal tube, and mechanically ventilated with 21% oxygen using a Healthdyne pediatric time-cycled, pressure-limited ventilator. With the use of strict aseptic technique, a midsternotomy incision was then performed. Patency of the vascular graft was confirmed by inspection and changes in oxygen saturation. A side-biting vascular clamp was used to isolate peripheral lung tissue from randomly selected lobes, and the incisions were cauterized. Approximately 300 mg of peripheral lung were obtained for each biopsy; four biopsies were obtained. Blood was obtained from the femoral artery.

At the end of the protocol, all lambs were killed with a lethal injection of pentobarbital sodium in accordance with the National Institutes of Health *Guidelines for the Care and Use of Laboratory Animals*. All protocols and procedures were approved by the Committees on Animal Research at the University of California, San Francisco, and the Medical College of Georgia.

Pulmonary arterial endothelial cell cultures. Primary cultures of juvenile ovine pulmonary arterial endothelial cells (PAEC) were isolated as detailed previously (68). All cultures were maintained in DMEM supplemented with 10% fetal calf serum (Hyclone, Logan, UT) and antibiotics/antimycotic solution (500 IU penicillin, 500 µg/ml streptomycin, and 1.25 µg/ml amphotericin B; MediaTech, Herndon, VA) at 37°C in a humidified atmosphere with 5% CO₂ and

95% air. Cells were used at *passages 9 and 10*, seeded at ~50% confluence, and utilized when fully confluent.

Western blot analysis. Lung protein extracts were prepared by homogenizing sheep lung tissues in lysis buffer (50 mM Tris·HCl, pH 7.6, 0.5% Triton X-100, and 20% glycerol) containing Halt protease inhibitor cocktail (Pierce, Rockford, IL). Extracts were then clarified by centrifugation (15,000 g for 15 min at 4°C). Supernatant fractions were assayed for protein concentration using the Bradford reagent (Bio-Rad, Richmond, CA) and used for Western blot analysis. Protein extracts (25–50 µg) were separated on LongLife 4–20% Tris-SDS-HEPES gels (Frenchs Forest, Australia) and electrophoretically transferred to Immuno-Blot polyvinylidene difluoride membrane (Bio-Rad Laboratories, Hercules, CA). The membranes were blocked with 5% nonfat dry milk in Tris-buffered saline containing 0.1% Tween 20. After blocking, the membranes were probed with antibodies to CrAT (Santa Cruz Biotechnology), CPT1-B (Affinity Bioreagents), CPT2 (Affinity Bioreagents), HSP90 (BD Transduction), MnSOD (Upstate, Lake Placid, NY), and uncoupling protein-2 (UCP-2; Calbiochem, La Jolla, CA). Reactive bands were visualized using chemiluminescence (SuperSignal West Femto substrate kit; Pierce) on a Kodak 440CF image station (New Haven, CT). Band intensity was quantified using Kodak 1D image processing software. Expression of each protein was normalized by stripping the blots with Restore Western blot stripping buffer (Pierce) and then reprobing them with β-actin as a loading control (Sigma, St. Louis, MO).

Measurement of carnitine homeostasis. Detection of carnitines was performed using an Amersham Biosciences AKTA purifier system (GE Healthcare, Piscataway, NJ) with a 5-µm OmniSpher C18 column (250 × 4.6-mm OD) equipped with a Jasco FP-2020 fluorescence detector (Tokyo, Japan). Total and free carnitines levels were quantified in lung tissue homogenates by fluorescence detection at 248 (excitation) and 418 nm (emission) as described previously (39, 43).

Sample purification and derivatization before HPLC detection. For free carnitine [L-carnitine and acetyl L-carnitine (ALCAR)] determination, 100-µl samples, 300 µl of water, and 100 µl of internal standard (Sigma ST 1093) were mixed. For total carnitine determination, 100-µl samples were hydrolyzed with 0.3 M KOH, heated at 45°C, and pH neutralized using perchloric acid; the volume was made to 400 µl, and 100 µl of internal standard was added. All samples were purified using solid-phase extraction columns (SAX, 100 mg/ml; Varian, Harbor City, CA), derivatized using aminoanthracene in the presence of EDCI (catalyst), and kept at 30°C for 1 h to complete reaction of carnitines. Separation was carried out with an isocratic elution in 0.1 M Tris-acetate buffer (pH 3.5)-acetonitrile (68:32, vol/vol) at a flow rate of 0.9 ml/min as described previously (39, 43).

Measurement of CrAT activity. Peripheral lung tissue was homogenized in 50 mM Tris·HCl, pH 7.5, 2 mM EDTA, 5 mM MgCl₂, 0.8 mM DTT, and 0.25 mM PMSF with protease inhibitor cocktail. The homogenates were then centrifuged at 3,500 g for 5 min, and Coomassie protein estimation was carried out. CrAT activity was then determined using a modification of the method described by Liu et al. (38). Briefly, the assay mixture consisted of 50 mM Tris·HCl, pH 7.5, 2 mM EDTA, 25 mM malate, 0.25 mM NAD, 12.5 g/ml rotenone, 0.04% Triton X-100, 12.5 g/ml malic dehydrogenase, 50 g/ml citrate synthase, 6.25 µM CoA, 200 µM CoA, 400 µM CoA, and 2 mM ALCAR. Sample (10 µl) with a protein concentration of 0.5 mg/ml was added to the assay mixture along with CoA (400 µM) with a constant concentration of 2 mM ALCAR (the *K_m* value for CoA). Reactions were monitored at room temperature for 5 min in a Beckman DU series 600 spectrophotometer. The absorbance was measured at time intervals of 30 s, giving 10 readings per sample. The rate was calculated using linear regression to determine the best-fit line.

Immunoprecipitation analysis for nitrated CrAT. To determine nitrated CrAT levels, we homogenized lung tissues in immunoprecipitation buffer [25 mM HEPES, pH 7.5, 150 mM NaCl, 1% Nonidet P-40, 10 mM MgCl₂, 1 mM EDTA, and 2% glycerol supplemented

with protease inhibitor cocktail (Pierce). Tissue homogenates (1,000 μ g of protein) were precipitated with a rabbit antibody against 3-nitrotyrosine (5 μ g; Upstate Biotechnology) in 0.5-ml final volume at 4°C overnight. Protein G plus/protein A agarose (40 μ l; Calbiochem) was added and rotated at 4°C for an additional 2 h. The precipitated protein was washed three times in 2 \times volume of immunoprecipitation buffer; the pellet was resuspended in Laemmli buffer (20 μ l), boiled, and separated on a 4–20% SDS-PAGE gel (LongLife). CrAT protein levels were then detected using Western blot analysis.

Determination of lactate and pyruvate levels. Lung tissues were homogenized in ice-cold 0.5 M perchloric acid and centrifuged at 14,000 rpm for 20 min. The supernatant were then neutralized with 3 M KHCO_3 and used for lactate and pyruvate assays. The relative changes in lactate levels were measured using a lactate assay kit (Biovision). Pyruvate levels were determined using the spectrophotometric enzymatic measurement assay at 340 nm. NADH was used as a cofactor and lactate dehydrogenase as the coenzyme. Experimental conditions were as previously described (40).

Immunoprecipitation analysis for HSP90 interaction with eNOS. For the experiments in PAEC, cells were treated with 50 μ M 2,4-dinitrophenol (2,4-DNP; Sigma) for up to 8 h. The cells were then lysed in ice-cold lysis buffer. For immunoprecipitation, cell lysates were incubated with anti-eNOS antibody (BD Transduction Laboratories) for 2 h at 4°C and then with protein G plus/protein A agarose suspension (Calbiochem) for 1 h at 4°C. The immune complexes were washed three times with the lysis buffer and boiled in SDS-PAGE sample buffer for 5 min. Agarose beads were pelleted by centrifugation, and protein supernatants were loaded and run on (4–20%) polyacrylamide gels, followed by transfer of the proteins to nitrocellulose membranes. Membrane was blocked with 2% BSA in Tris-buffered saline containing 0.05% Tween 20 (TBST) for 2 h at room temperature, incubated with anti-HSP90 (BD Transduction Laboratories) for 2 h at room temperature, washed three times with TBST (room temperature, 10 min), and then incubated with a horseradish peroxidase-conjugated secondary antibody (Pierce). The reactive bands were visualized with the SuperSignal West Femto maximum sensitivity substrate kit (Pierce) and Kodak 440CF image station. The same blot was reprobed with anti-eNOS antibody to normalize for the levels of eNOS immunoprecipitated in each sample.

To determine eNOS-HSP90 interactions in the peripheral lung, tissues were homogenized in immunoprecipitation buffer as described above for nitrated CrAT. Tissue homogenates (1,000 μ g of protein) were then analyzed as described for PAEC.

Shear stress. Laminar shear stress was applied using a cone-plate viscometer that accepts six-well tissue culture plates, as described previously (15, 67, 69). This method achieves laminar flow rates that represent physiological levels of laminar shear stress in the major human arteries, which is in the range of 5–20 dyn/cm^2 with localized increases to 30–100 dyn/cm^2 .

Determination of mitochondrial dysfunction in PAEC. We utilized two measures to identify mitochondrial dysfunction in PAEC exposed to 2,4-DNP. First, we determined the effect of 2,4-DNP (50 μ M, 0–8 h) on PAEC ATP generation. ATP levels were estimated using the firefly luciferin-luciferase method with a commercially available kit (Invitrogen). Luminescence was determined using a Fluoroscan Ascent FL plate luminometer (Thermo Electron). Values for untreated cells at *time 0* were set to 100%, and time-dependent changes in ATP levels were reported as a percentage of the value at *time 0*.

Second, we determined the effect on mitochondrial superoxide production using the MitoSOX red mitochondrial superoxide indicator (Molecular Probes), a fluorogenic dye for selective detection of superoxide in the mitochondria of live cells. MitoSOX red reagent is live-cell permeant and is rapidly and selectively targeted to the mitochondria. Once in the mitochondria, MitoSOX red reagent is oxidized by superoxide and exhibits bright red fluorescence upon binding to nucleic acids. Briefly, after treatment with 2,4-DNP, cells

were washed with fresh medium and then incubated in medium containing MitoSOX red (2 μ M) for ~10 min at 37°C in dark conditions. Cells were washed with fresh serum-free medium and imaged using fluorescence microscopy at an excitation of 510 nm and an emission of 580 nm. A personal computer-based imaging system consisting of the following components was used for the fluorescent analyses: an Olympus IX51 microscope equipped with a charge-coupled device camera (Hamamatsu Photonics) was used for acquisition of fluorescent images. The average fluorescence intensities (to correct for differences in cell number) were quantified using ImagePro Plus version 5.0 imaging software (Media Cybernetics).

Detection of NO_x levels in PAEC. NO generated by PAEC in response to shear was measured using an NO-sensitive electrode with a 2-mm-diameter tip (ISO-NOP sensor; WPI) connected to an NO meter (ISO-NO Mark II; WPI) as described previously (70).

Measurement of tissue NO_x levels. To quantify bioavailable NO, we determined levels of NO and its metabolites in the peripheral lung tissue from shunt and age-matched control lambs at 4 wk of age. In solution, NO reacts with molecular oxygen to form nitrite and with oxyhemoglobin and superoxide anion to form nitrate. Nitrite and nitrate are reduced using vanadium(III) and hydrochloric acid at 90°C. NO is purged from solution, resulting in a peak of NO for subsequent detection by chemiluminescence (NOA 280; Sievers Instruments, Boulder, CO). The detection limit is 1 nM per milliliter of nitrate.

Electron paramagnetic resonance spectroscopy and spin trapping. To detect superoxide generation in intact cells, we performed electron paramagnetic resonance (EPR) measurements as described previously (70). After overnight serum starvation of the cells, 20 μ l of spin-trap stock solution consisting of 1-hydroxy-3-methoxycarbonyl-2,2,5,5-tetramethylpyrrolidine·HCl (CMH; Alexis Biochemicals, San Diego, CA) at 20 μ M in Dulbecco's PBS (DPBS) plus 25 μ M desferrioxamine (Calbiochem) and 5 μ M diethyldithiocarbamate (Alexis Biochemicals, Lausen, Switzerland) plus 2 μ l of DMSO were added to each well before shear stimulation. Adherent cells were trypsinized and pelleted at 500 g after 45 min of incubation at 37°C following shear to allow entrapment of superoxide by the spin trap. Cell pellet was washed and suspended in a final volume of 35 μ l of DPBS (plus desferrioxamine and diethyldithiocarbamate), loaded into a 50- μ l capillary tube, and analyzed with a MiniScope MS200 EPR (Magnetech, Berlin, Germany) at a microwave power of 40 mW, modulation amplitude of 3,000 mG, and modulation frequency of 100 kHz. EPR spectra were analyzed measured for amplitude using ANALYSIS software (version 2.02; Magnetech), and experimental groups were compared using the statistical analysis described below.

Measurement of superoxide levels in peripheral lung tissue. Approximately 0.2 g of peripheral lung tissue was sectioned from fresh frozen tissue and immediately immersed in either normal EPR buffer [PBS supplemented with 5 μ M diethyldithiocarbamate (Sigma-Aldrich) and 25 μ M desferrioxamine (Sigma-Aldrich)] or EPR buffer supplemented with 100 U/ml polyethylene glycol-superoxide dismutase (PEG-SOD; Sigma) or 100 μ M 3-ethylisothiourea (ETU; Sigma), an inhibitor of human NO synthases (21). Samples were incubated for 30 min on ice. During incubation, samples were analyzed for protein content using Bradford analysis (Bio-Rad). Sample volumes were then adjusted with EPR buffer plus 25 mg/ml CMH hydrochloride (Axxora) to achieve equal protein content and a final CMH concentration of 5 mg/ml. Samples were homogenized for 30 s with a VWR PowerMAX AHS 200 tissue homogenizer, incubated for 60 min on ice, and then centrifuged at 14,000 g for 15 min at room temperature. Supernatant (35 μ l) was loaded into a 50- μ l capillary tube and analyzed for superoxide generation as described above.

To demonstrate that ETU quenched superoxide in a nonspecific manner within our experimental system, we utilized an *in vitro* superoxide-creating reaction of xanthine oxidase (1 U/ml; Sigma) with xanthine (1 mM; Sigma), as previously described (29) in the presence of CMH hydrochloride. Reactions were run in a total volume of 1 ml (PBS, pH 7.5) for 20 min at 25°C. Two control reactions, one

lacking xanthine and the other lacking xanthine oxidase, were included to ensure the absence of nonspecific reactions of either reagent with the EPR spin trap. After incubation, 35 μ l of supernatant were loaded into a 50- μ l capillary tube and analyzed for superoxide generation as described above.

Statistical analyses. Statistical analysis was performed using GraphPad Prism version 4.01 for Windows (GraphPad Software, San Diego, CA). Means \pm SE were calculated for all samples, and significance was determined using the unpaired *t*-test (for 2 groups) or ANOVA (for ≥ 3 groups). A value of *P* < 0.05 was considered significant.

RESULTS

Increased pulmonary blood flow in shunt lambs. All shunt lambs had a palpable thrill and an increase in the oxygen saturation between the right ventricle and pulmonary artery, demonstrating patency of the graft. In fact, the pulmonary-to-systemic blood flow ratio of shunt lambs was 2.9 ± 0.9 . Compared with 2-wk-old control lambs, 2-wk-old shunt lambs had increased mean pulmonary arterial pressure (21.7 ± 3.2 vs. 15.3 ± 2.3 mmHg), left pulmonary blood flow (147.3 ± 23.4 vs. 55.1 ± 13.2), and left atrial pressure (6.8 ± 3.7 vs. 2.7 ± 1.6 mmHg) (*P* < 0.05). Right atrial pressure, heart rate, and mean systemic arterial pressure values were similar between the groups.

Reduced expression of the enzymes involved in carnitine homeostasis in shunt lambs. Initially, we measured the expression of the three important mitochondrial enzymes involved in carnitine metabolism: CPT1-B, CPT2 (involved in the transport of long-chain fatty acids from cytosol to mitochondrial matrix), and CrAT (transesterifies short-chain acyl chains) in 2-wk old shunt and age-matched control lambs. There was a significant decrease in the expression of both CPT1-B (Fig. 1, A and B) and CPT2 enzymes (Fig. 1, C and D) in shunts compared with age-matched control lambs. Similarly, both CrAT expression (Fig. 2, A and B) and activity (control: 152.9 ± 46.1 units/mg vs. shunt: 7.43 ± 3.33 units/mg, *P* < 0.05 vs. control; Fig. 2C) were significantly decreased in shunt compared with age-matched control lambs.

Increased nitration decreases CrAT activity in shunt lambs. Although our data indicated that CrAT expression was decreased ~ 2 -fold, the CrAT activity was decreased ~ 20 -fold. This suggested that a posttranslational modification was altering CrAT activity. Since we had previously found that there is an increase in oxidative stress in the shunt lambs, we focused on the potential role of enzyme nitration. The levels of nitrated CrAT were determined using immunoprecipitation with a specific antiserum raised against 3-nitrotyrosine residues and were found to be significantly increased in shunt compared with age-matched control lambs (Fig. 3, A and B). Furthermore, we found that exposing purified CrAT to peroxynitrite (10 μ M, 5 min) was sufficient to significantly reduce CrAT activity (vehicle: 99.9 ± 17.74 units/ μ g vs. peroxynitrite: 0.6481 ± 0.24 units/ μ g, *P* < 0.05 vs. vehicle; Fig. 4).

Decreased CrAT activity leads to alterations in carnitine metabolism. CrAT plays an important role in maintaining carnitine metabolism (10). Therefore, we next determined total carnitine and free carnitine levels in the peripheral lung of shunt and control lambs. Using HPLC analysis, we found that total carnitine levels were unchanged in shunt lambs (60.54 ± 8.45 vs. 72.37 ± 10.14 nmol/g wet wt; Table 1). However, free carnitine levels were decreased (34.86 ± 3.35 vs. 67.57 ± 13.43 nmol/g wet wt, *P* < 0.05 vs. control; Table 1). Furthermore, L-carnitine levels were significantly lower in shunt compared with age-matched control lambs (20.21 ± 4.29 vs. 56.41 ± 12.27 nmol/g wet wt, *P* < 0.05 vs. control; Table 1). Since free carnitines and other acylcarnitines contribute to total carnitine levels, these data indicate that the percentage of carnitine present as acylcarnitine (calculated as total carnitine minus free carnitine) is significantly higher in shunt lambs (40.71 ± 9 vs. $6.2 \pm 4.7\%$, *P* < 0.05 vs. control; Table 1).

Altered carnitine metabolism is associated with mitochondrial dysfunction in shunt lambs. Since the carnitine acyltransferase pathway has been shown to be of critical importance for maintaining normal mitochondrial function, we next determined whether shunt lambs present with markers of mitochon-

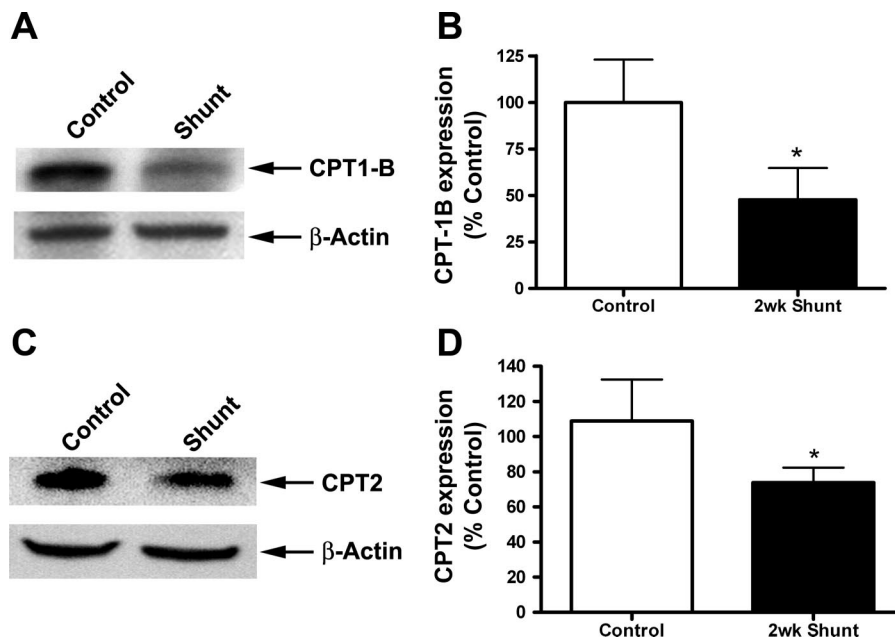
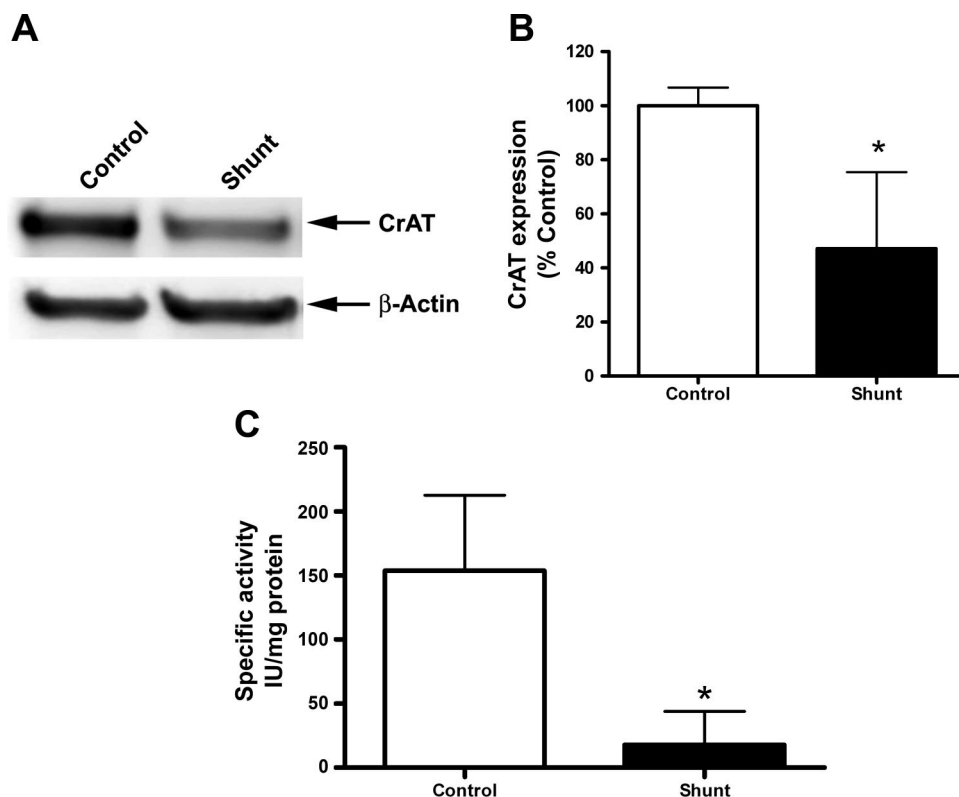


Fig. 1. Carnitine palmitoyltransferase (CPT) expression in peripheral lung tissue from control and shunt lambs at 2 wk of age. **A:** protein extracts (50 μ g) prepared from peripheral lung of shunt and control lambs were analyzed by Western blot analysis using a specific antiserum raised against CPT1-B protein. CPT1-B expression was also normalized for loading using β -actin. A representative blot is shown. **B:** there was a significant decrease in normalized densitometric values for CPT1-B protein in peripheral lung tissue prepared from shunt compared with control lambs. Values are means \pm SE; *n* = 6 control and 6 shunt lambs. **P* < 0.05 vs. control. **C:** protein extracts (50 μ g) prepared from peripheral lung of shunt or control lambs were analyzed by Western blot analysis using a specific antiserum raised against CPT2 protein. CPT2 expression was also normalized for loading using β -actin. A representative blot is shown. **D:** there was a significant decrease in normalized densitometric values for CPT2 protein in peripheral lung tissue prepared from shunt compared with control lambs. Values are means \pm SE; *n* = 6 control and 6 shunt lambs. **P* < 0.05 vs. control.

Fig. 2. Carnitine acetyltransferase (CrAT) expression and activity in peripheral lung tissue from control and shunt lambs at 2 wk of age. **A**: protein extracts (50 μ g) prepared from peripheral lung of shunt and control lambs were analyzed by Western blot analysis using a specific antiserum raised against CrAT protein. CrAT expression was also normalized for loading using β -actin. A representative blot is shown. **B**: there was a significant decrease in normalized densitometric values for CrAT protein in peripheral lung tissue prepared from shunt compared with control lambs. Values are means \pm SE; $n = 6$ control and 6 shunt lambs. $*P < 0.05$ vs. control. **C**: CrAT activity was determined in protein extracts (40 μ g) prepared from peripheral lung tissue from control and shunt lambs. There was a significant decrease in CrAT activity in peripheral lung tissue prepared from shunt compared with control lambs. Values are expressed as units of activity per μ g of protein and are means \pm SE; $n = 4$ control and 4 shunt lambs. $*P < 0.05$ vs. control.



drial dysfunction. Because loss of SOD2 (8, 13, 18, 26, 35, 44, 48) and increases in UCP-2 (2, 27, 42, 46, 62) have been shown to be markers of mitochondrial dysfunction in other systems, we examined these markers. Our data indicate that SOD2 expression was significantly decreased (Fig. 5, *A* and *B*) in shunt lambs, whereas UCP-2 expression was significantly increased (Fig. 5, *C* and *D*). In addition, we determined the lung levels of lactate and pyruvate in shunt and control lambs to quantify mitochondrial activity. Under normal mitochondrial function, pyruvate levels are higher than lactate, and thus any increases in lactate levels decreases the pyruvate-to-lactate ratio and can be extrapolated to suggest a reduction in ATP generation by the mitochondria (57). As shown in Table 2, shunt lambs had significantly decreased pyruvate levels (0.059 ± 0.007 vs. 0.132 ± 0.028 μ mol/g wet wt, $P < 0.05$)

and increased lactate levels (0.568 ± 0.838 vs. 1.348 ± 0.214 μ mol/g wet wt, $P < 0.05$) as well as a significant reduction in the pyruvate-to-lactate ratio.

Mitochondrial dysfunction attenuates HSP90-eNOS interaction and shear-induced NO production in PAEC. To further investigate the effect of mitochondrial dysfunction on NO signaling, we utilized cultured PAEC isolated from juvenile lambs. Mitochondrial dysfunction was induced in PAEC by using 2,4-DNP (50 μ M, 0–6 h). Our data indicate that 2,4-DNP significantly decreased ATP levels in PAEC (Fig. 6*A*) associated with an increase in oxidative stress within the mitochondria (Fig. 6*B*). Furthermore, we found that this mitochondrial dysfunction was associated with a decrease in the association of HSP90 with eNOS (Fig. 7, *A* and *B*) and shear-induced NO production (Fig. 7*C*) and an increase in eNOS-

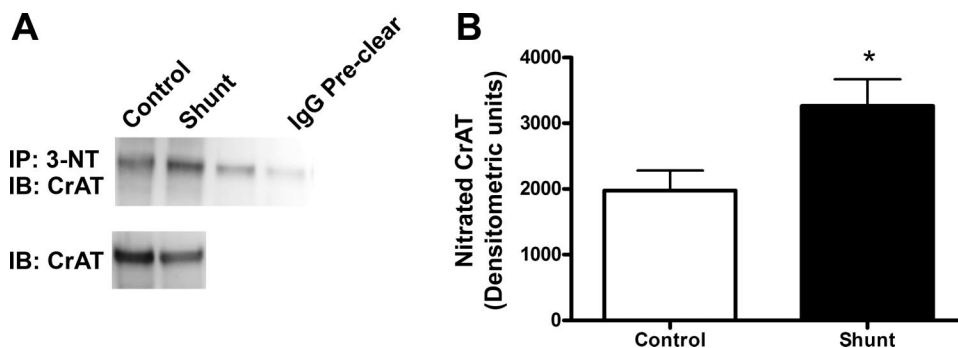


Fig. 3. Increased nitration of CrAT in peripheral lung tissue of shunt lambs at 2 wk of age. **A**: protein extracts (1,000 μ g) prepared from peripheral lung of shunt and control lambs were subjected to immunoprecipitation (IP) using an antibody specific to 3-nitrotyrosine (3-NT) and then analyzed by Western blot analysis using a specific antiserum raised against CrAT protein. A representative immunoblot (IB) is shown with CrAT expression. Minimal binding was observed in the beads alone or in IgG pre-clear. **B**: there was a significant increase in nitrated CrAT protein in peripheral lung tissue prepared from shunt compared with control lambs. Values are means \pm SE; $n = 6$ control and 6 shunt lambs. $*P < 0.05$ vs. control.

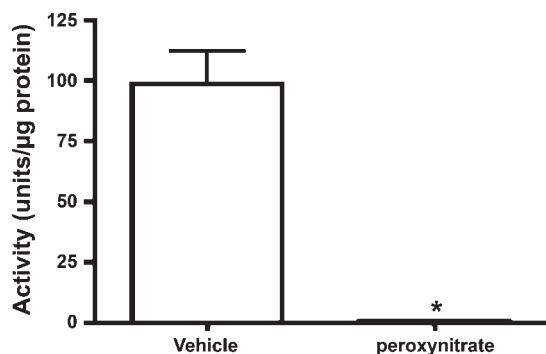


Fig. 4. Peroxyntirite decreases CrAT activity. Purified pigeon breast muscle CrAT was exposed to authentic peroxyntirite or vehicle, and then the activity was determined. Peroxyntirite induced a significant decrease in CrAT activity. Values are means \pm SD; $n = 6$. * $P < 0.05$ vs. vehicle.

derived superoxide (Fig. 7D), indicating that impaired mitochondrial function reduces NO production.

Decreased HSP90-eNOS interaction and altered NO signaling in shunt lambs. To determine the effect of decreased mitochondrial function in shunt lambs on NO signaling, we carried out immunoprecipitation studies to determine eNOS-HSP90 interactions in both 2- and 4-wk-old shunt and control lambs. Our data indicate that there was a progressive decrease in eNOS-HSP90 interactions between 2 and 4 wk of age in shunt compared with control lambs (Fig. 8, A and B) and that this was associated with a progressive decrease in relative eNOS activity (as determined by tissue NO_x levels as a fraction of calcium-dependent [^3H]arginine metabolism, Fig. 8C) and increased NOS-dependent superoxide levels indicative of eNOS uncoupling (Fig. 8D). We also confirmed the specificity of ETU for NOS-derived superoxide by demonstrating that ETU did not quench the superoxide generated by a xanthine/xanthine oxidase superoxide-generating system (Fig. 8E).

DISCUSSION

The important findings of this study are that 1) decreased expression and activity of mitochondrial enzymes involved in carnitine metabolism in 2-wk-old shunt lambs causes disruption of carnitine homeostasis, leading to mitochondrial dysfunction; and 2) decreased mitochondrial function leads to a progressive disruption of HSP90-eNOS interaction, leading to decreased NO signaling in shunt lambs. Thus this study provides insight into a novel mechanism that may be involved in the development of pulmonary hypertension whereby the disruption of carnitine metabolism leads to mitochondrial dysfunction and endothelial dysfunction.

The mitochondrial membrane is impermeable to long-chain fatty acids, and carnitine is required for transportation of these fatty acids into the mitochondria for β -oxidation. Carnitine is present in the form of either free carnitine (nonesterified molecule; FC), or acylcarnitines (esterified form; AC). Cytosolic long-chain fatty acids that are present as CoA esters are transesterified to L-carnitine in a reaction catalyzed by the CPT1 enzyme at the inner aspect of the mitochondrial outer membrane, converting long-chain acyl-CoA to long-chain acylcarnitine (64). At the inner mitochondrial membrane, acylcarnitine is transesterified back to free carnitine and long-chain acyl-CoA, a reaction catalyzed by CPT2, situated on the matrix

side of the inner mitochondrial membrane (71). Thus transfer of fatty acids into the mitochondria is dependent on the function of the CPT enzymes. In this study we found decreased expression of both CPT1 and CPT2 enzymes in shunt lambs, suggesting that β -oxidation may be disrupted. Indeed, CPT deficiencies are common disorders of mitochondrial fatty acid oxidation. For example, CPT2 deficiency in infants causes severe attacks of hypoketotic hypoglycemia, occasionally associated with cardiac damage, and is commonly responsible for sudden death before 1 yr of age (9).

Another important mitochondrial enzyme, CrAT, which resides in the matrix, is able to reconvert the short- and medium-chain acyl-CoAs into acylcarnitines by using intramitochondrial carnitine. Through this mechanism of reversible acylation, carnitine is able to modulate the intracellular concentrations of free CoA and acyl-CoA (64). Cell-based and in vivo studies from the Ames group have implicate damage to the CrAT enzyme that may decrease its affinity for carnitine (36–38). Decreased CrAT activity leads to increased levels of acyl-CoA, which leads to inhibition of multiple enzymatic processes involved in oxidative metabolism. We found that CrAT expression was decreased \sim 2-fold in shunt lambs but that CrAT activity was decreased \sim 20-fold, suggesting a posttranslational inhibitory mechanism was also involved. Utilizing immunoprecipitation analysis, we also investigated CrAT nitration levels. We found that CrAT nitration was higher in shunt lambs relative to controls. Furthermore, in vitro we observed that exposure to peroxyntirite reduced the activity of the native protein. Together, our data suggest that the nitration of CrAT is likely to be more important with respect to the decrease in CrAT activity than decreased gene expression. However, it should be noted that although decreased CrAT activity will decrease carnitine metabolism, other substrates are also involved in this reaction, such as acetyl-CoA, whose generation requires fatty acid oxidation. Thus it is possible that the alterations we have observed in CrAT activity may only partly account for the alterations in carnitine homeostasis in the shunt lung. However, further studies are required to investigate this possibility.

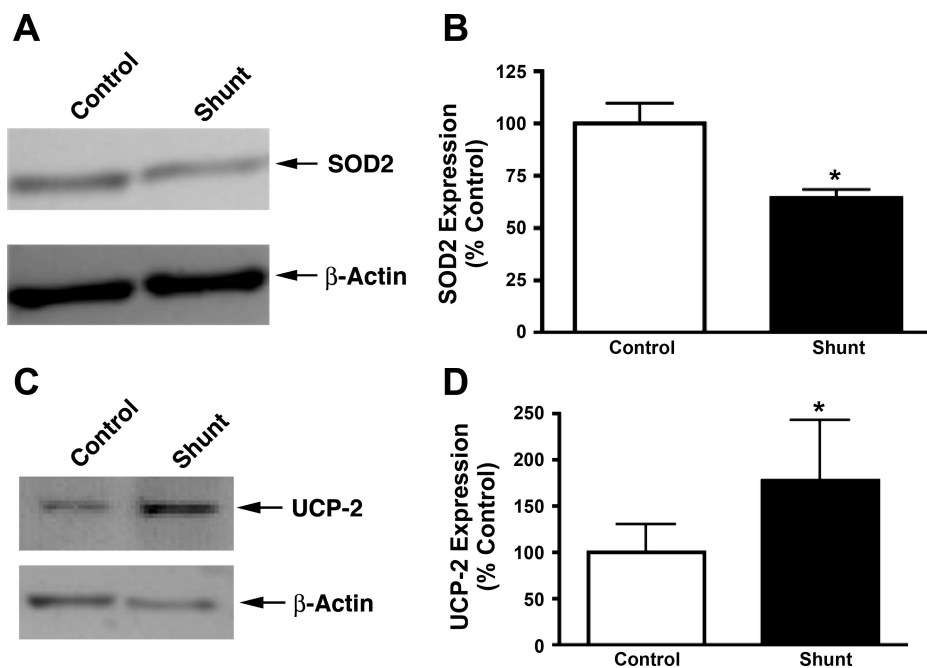
Carnitine availability becomes a limiting step for β -oxidation in certain physiological and pathological diseases, and carnitine supplementation enhances fatty acid metabolism in the mitochondria, restoring normal mitochondrial function by maintaining the equilibrium between acyl-CoA and free CoA (63). The levels of acylcarnitines are increased in plasma of patients with several inherited metabolic diseases. In these cases, the endogenous pool of carnitine becomes insufficient to cope with the required acyl transfer, and the plasma AC/FC ratio increases (10). The increase in AC/FC ratio reflects changes in the intramitochondrial equilibrium between acyl-CoA and free CoA (7, 12). Increase in this ratio indicates

Table 1. Carnitine levels in peripheral lungs of shunt and control lambs

	Total Carnitines, nmol/g wet wt	Free Carnitine, nmol/g wet wt	L-Carnitine, nmol/g wet wt	Acylcarnitine, % of total
Control	60.54+8.45	67.57+13.43	56.42+12.27	6.2+4.7
Shunt	72.37+10.14	34.86+3.35*	20.21+4.29*	40.71+9*

Data are means \pm SE; $n = 5$. * $P < 0.05$ vs. control.

Fig. 5. Markers of mitochondrial dysfunction are increased in shunt lambs at 2 wk of age. **A:** protein extracts (25 μ g) prepared from peripheral lung of shunt and control lambs were analyzed by Western blot analysis using a specific antiserum raised against SOD2 protein. SOD2 expression was also normalized for loading using β -actin. A representative blot is shown. **B:** there was a significant decrease in normalized densitometric values for SOD2 protein in peripheral lung tissue prepared from shunt compared with control lambs. Values are means \pm SE; $n = 6$ control and 6 shunt lambs. $*P < 0.05$ vs. control. **C:** protein extracts (25 μ g) prepared from peripheral lung of shunt and control lambs were analyzed by Western blot analysis using a specific antiserum raised against uncoupling protein-2 (UCP-2). UCP-2 expression was also normalized for loading using β -actin. A representative blot is shown. **D:** there was a significant increase in normalized densitometric values for UCP-2 protein in peripheral lung tissue prepared from shunt compared with control lambs. Values are means \pm SE; $n = 6$ control and $n = 6$ shunt lambs. $*P < 0.05$ vs. control.



accumulation of acyl-CoA or reduction in FC and is associated with compromise of mitochondrial metabolism (7). More recent data have shown that under conditions of metabolic stress, mitochondria accumulate acyl-CoA, which is normally maintained in homeostasis with carnitine. High acyl-CoA levels inhibit multiple enzymatic processes involved in oxidative metabolism (14). This product can inhibit multiple other mitochondrial enzymes downstream from its own synthesis, resulting in a metabolic roadblock within the mitochondrial matrix (41, 49, 58, 61). In our lamb model, the AC/FC ratio was higher in 2-wk shunt compared with age-matched control lambs, indicating decreased mitochondrial function and impaired fatty acid metabolism. If disruption in carnitine metabolism is an important contributing factor in the development of endothelial dysfunction, then treatment with carnitine may attenuate at least in part any endothelial injury associated with the development of pulmonary hypertension and could be used as an effective therapeutic agent for the prevention of the mitochondrial dysfunction associated in pulmonary hypertension. Indeed, a recent study has shown that in neonatal rats, hypoxia-ischemia is associated with a significant increase in acyl-CoA/CoA ratio, and this imbalance can be prevented by treatment with exogenous carnitine (66).

SOD2 is an important mitochondrial enzyme regulating the redox level within the mitochondrion by scavenging the free radicals produced in the mitochondria. Reduction of SOD2 protein expression is widely considered to be a hallmark of decreased mitochondrial function (8, 13, 18, 26, 35, 44, 48). Our data show a significant reduction in SOD2 expression in shunt compared with age-matched control lambs, again supporting the notion of mitochondrial dysfunction in the shunt lambs. In addition to SOD2, we examined expression of another important mitochondrial protein, UCP-2, in both control and shunt lambs. UCP-2 is a mitochondrial membrane proton transporter that mediates proton leak across the inner mitochondrial membrane, reducing the energy force for cellu-

lar ATP production (32, 51). As with a decrease in SOD2, an increase in UCP-2 expression is thought to be a marker for mitochondrial dysfunction (2, 27, 42, 46, 62). For example, UCP-2 is found to be upregulated in islets of mouse in a model of obesity-induced diabetes, where superoxide-mediated activation of UCP-2 has been shown to play an important role in the pathogenesis of β -cell dysfunction (33). Our data demonstrated a significant increase in UCP-2 expression in shunt compared with age-matched control lambs, again supporting the notion of mitochondrial dysfunction in the shunt lambs. Further support for this comes from our examination of lactate and pyruvate levels in lung tissue in shunt and age-matched control lambs. When pyruvate is not utilized by mitochondria for energy production, it gets converted into lactate. A higher lactate/pyruvate ratio is correlated with many pathological conditions related to mitochondria. We found higher lactate levels and an increased lactate/pyruvate ratio in our shunt lamb model. Together, our data demonstrating decreases in SOD2 and increases in UCP-2-expression and the increased lactate/pyruvate ratio indicate that shunt lambs have decreased mitochondrial function.

Mitochondria play essential physiological roles in cells and are the major site of cellular ATP production. Decreased mitochondrial function results in reduced ATP production and increased ROS generation with deleterious effects. Disruption of mitochondrial function is a critical event in a number of pathological conditions, including hypoxia-ischemic injuries (6), stroke (59), and diabetes (16, 45, 47, 50). There is also

Table 2. Lactate and pyruvate levels in peripheral lungs of shunt and control lambs

	Lactate, μ mol/g wet wt	Pyruvate, μ mol/g wet wt	Lactate/Pyruvate Ratio
Control	1.79 \pm 0.34	0.144 \pm 0.03*	15.25 \pm 4.35:1
Shunt	3.1 \pm 0.86*	0.057 \pm 0.008*	51.8 \pm 10.92:1*

Data are means \pm SE; $n = 5$. $*P < 0.05$ vs. control.

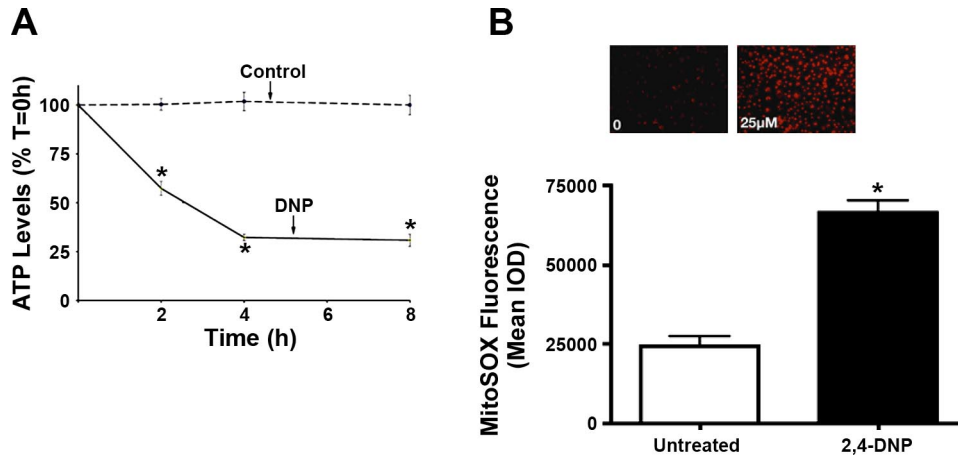


Fig. 6. 2,4-Dinitrophenol (2,4-DNP) decreases ATP levels and increases mitochondrial oxidative stress in pulmonary arterial endothelial cells (PAEC). *A*: PAEC were treated with 2,4-DNP (25 μ M, 0–8 h), and the cellular ATP levels were then determined. 2,4-DNP significantly decreased cellular ATP levels. Values are means \pm SE; $n = 6$. *T*, time. $*P < 0.05$ vs. control. *B*: PAEC were treated with 2,4-DNP (25 μ M, 4 h). Cells were then exposed to MitoSox (10 μ M, 15 min) to measure mitochondrial superoxide levels (as a marker for mitochondrial dysfunction). 2,4-DNP induced a significant increase in MitoSox fluorescence (representative images are shown as an inset). Values are means \pm SE; $n = 4$. $*P < 0.05$ vs. untreated.

considerable evidence for decreased mitochondrial function in aging-related neurodegenerative disorders (17, 22). Furthermore, previous studies have shown the importance of ATP in the pulmonary system as demonstrated by its key role in the birth-related pulmonary vasodilation in fetal lambs (30, 31), while a study in poultry has shown that lung mitochondrial dysfunction is present in broilers with pulmonary hypertension syndrome associated with oxidative stress (28). The role of ATP in endothelial function may be due, at least in part, to its ability to stimulate NO release via the activation of eNOS (30, 31). HSP90, a molecular chaperone, modulates the eNOS

activity (19, 20). It has been demonstrated that eNOS can interact with a 90-kDa heat shock protein (HSP90). HSP90 is part of a family that acts as molecular chaperones that can modulate protein activity. HSP90 appears to increase eNOS activity by facilitating the calmodulin-induced displacement of caveolin 1 from eNOS (24), which is inhibited with the HSP90 inhibitor geldamycin (20). HSP90 is ATP dependent, and the ATPase site of the chaperone is responsible for the auto phosphorylation required to enable HSP90 to interact with client proteins (54, 55). Interaction of HSP90 with eNOS has been shown to increase eNOS activity and NO production,

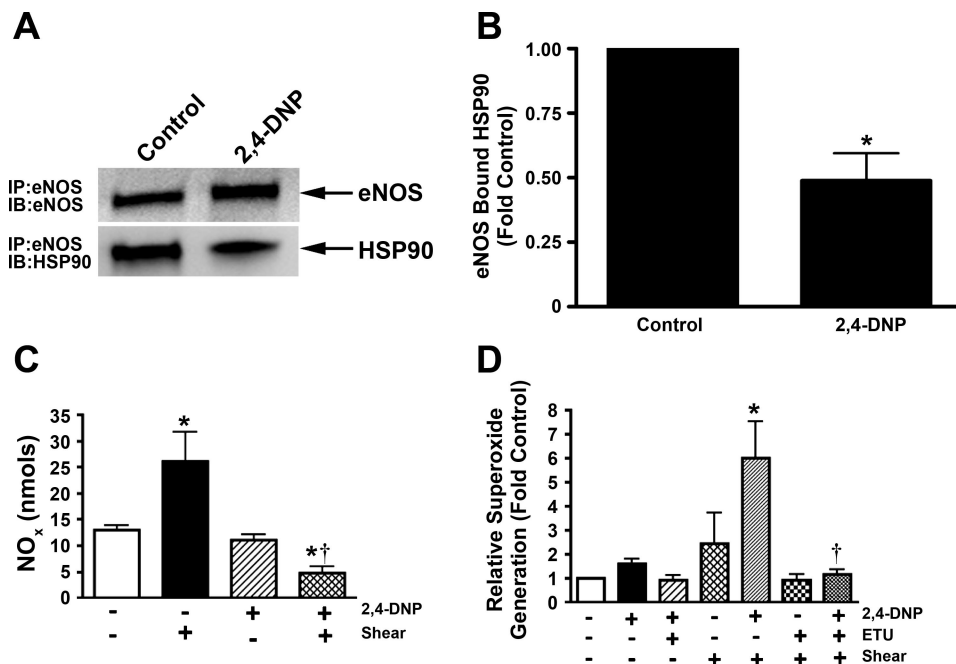


Fig. 7. 2,4-DNP decreases NO signaling in PAEC. *A*: PAEC were treated with 2,4-DNP (25 μ M, 4 h) and washed with PBS, and lysates were prepared with modified RIPA buffer. IP was performed using an antibody to endothelial nitric oxide synthase (eNOS) and then Western blot analysis was done using a specific antiserum raised against heat shock protein 90 (HSP90). Blots were also stripped and reprobed for eNOS to normalize the IP. A representative blot is shown. *B*: 2,4-DNP treatment caused a significant reduction in eNOS-HSP90 interaction. Values are means \pm SE; $n = 3$. $*P < 0.05$ vs. untreated. *C*: cells were treated with 2,4-DNP (25 μ M, 4 h) and exposed to laminar shear stress (20 dyn/cm², 15 min), and then the medium was assayed for nitrate/nitrite (NO_x) as an indirect determination of NO production. 2,4-DNP significantly decreased the shear-mediated increase in NO_x. Values are means \pm SE; $n = 6$. $*P < 0.05$ vs. no shear. $\dagger P < 0.05$ vs. control. *D*: cells were treated with 2,4-DNP (25 μ M, 4 h) in the presence and absence of the NOS inhibitor 3-ethylisothiourea (ETU; 100 μ M) and then exposed to laminar shear stress (20 dyn/cm², 15 min). Superoxide levels were then determined using the spin trap 1-hydroxy-3-methoxycarbonyl-2,2,5,5-tetramethylpyrrolidine·HCl. 2,4-DNP significantly increased NOS-dependent superoxide generation in response to shear. Values are means \pm SE; $n = 3$. $*P < 0.05$ vs. no shear. $\dagger P < 0.05$ vs. shear + 2,4-DNP.

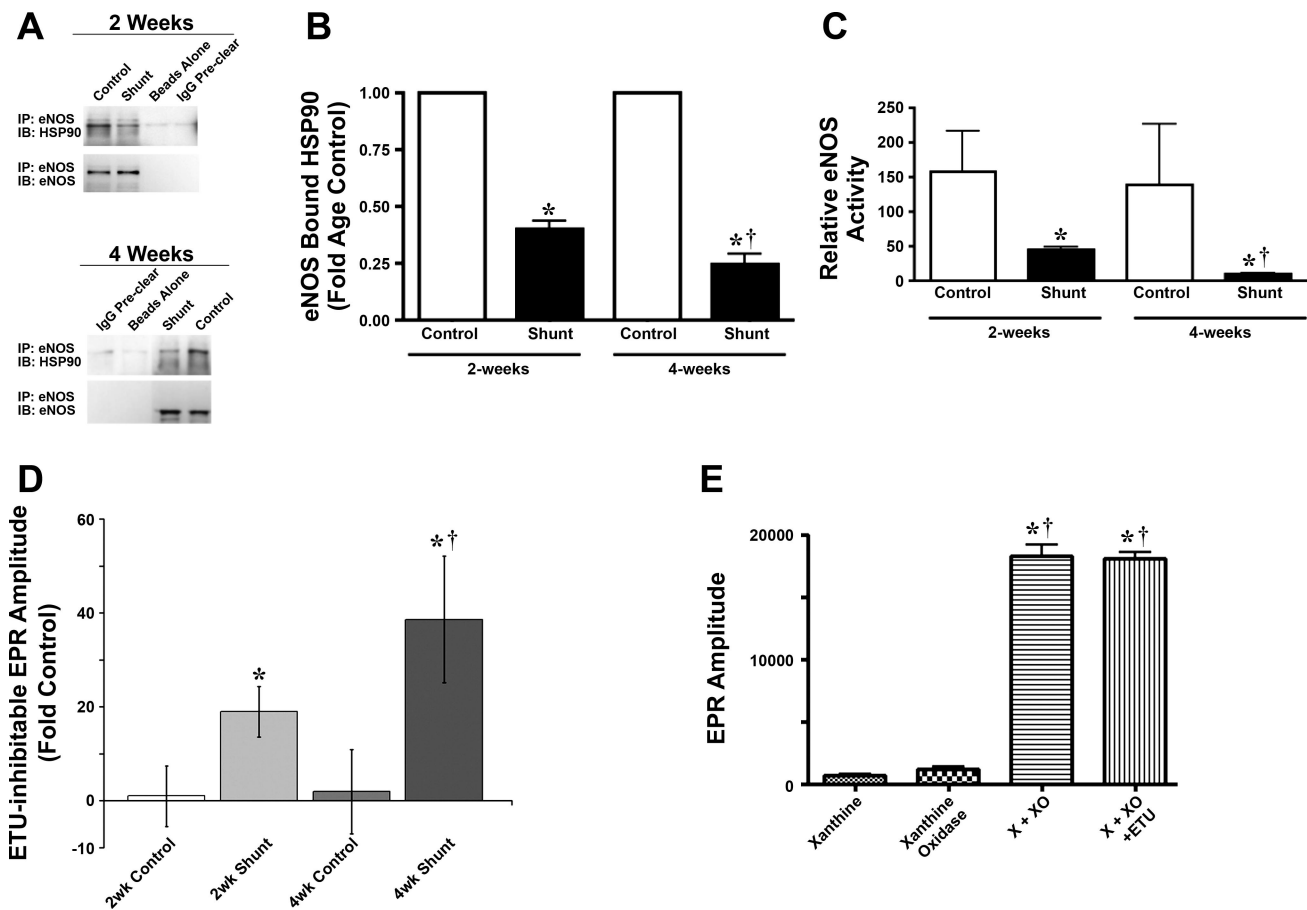


Fig. 8. Progressive decreases in the interaction of eNOS with HSP90 in shunt compared with control lambs. *A*: the interaction of eNOS with HSP90 was determined by IP using specific antiserum raised against eNOS in tissue extracts prepared from peripheral lung of shunt and control lambs at 2 and 4 wk of age. IP extracts were analyzed using antisera against either eNOS or HSP90. A representative image is shown. No specific protein bands were observed in the beads alone or in IgG pre-clear. *B*: the levels of eNOS protein associated with HSP90 relative to total eNOS protein were calculated. The data obtained indicate that there was a progressive decrease in the association of eNOS with HSP90 in shunt compared with control lambs between 2 (bars at left) and 4 wk of age (bars at right). Values are means \pm SE; $n = 5$ shunt and 5 control lambs at each age. * $P < 0.05$ compared with age-matched control. † $P < 0.05$ vs. 2-wk shunt. *C*: relative eNOS activity was estimated in shunt and age-matched control lambs at 2 and 4 wk of age by dividing peripheral lung tissue NO_x levels by total lung eNOS activity (determined by calcium-dependent [^3H]arginine to [^3H]citrulline conversion). Relative eNOS activity was significantly lower in the shunt lambs at both 2 and 4 wk of age. Values are means \pm SE; $n = 4$ shunt and 4 control lambs at each age. * $P < 0.05$ compared with age-matched control. † $P < 0.05$ vs. 2-wk shunt. *D*: superoxide anion levels determined by electron paramagnetic resonance (EPR) in snap-frozen lung tissue from shunt and age-matched control lambs at 4 wk of age in the presence and absence of the NOS inhibitor ETU (100 μM). A bar graph representing the cumulative data is shown. ETU-inhibitable superoxide levels were significantly higher in the shunt lambs. Values are means \pm SD; $n = 6$ shunt and 6 control lambs at each age. * $P < 0.05$ compared with age-matched control. † $P < 0.05$ vs. 2-wk shunt. *E*: superoxide was generated in vitro by cross-reacting xanthine oxidase (XO; 1 U/ml) with xanthine (X; 1 mM) in the presence or absence of ETU (100 μM). Two control reactions, one lacking X and the other lacking XO, were included to ensure the absence of nonspecific reactions of either reagent with the EPR spin trap. The significant increase in superoxide generated by the X/XO reaction was not significantly quenched by the presence of ETU. Values are means \pm SE; $n = 3$ for each condition. * $P < 0.05$ compared with X alone. † $P < 0.05$ vs. XO alone.

whereas decreased association of eNOS with HSP90 leads to enhanced eNOS-dependent production of superoxide (52). In the present study, we have shown that mild mitochondrial inhibition with the mitochondrial uncoupler 2,4-DNP caused a sustained decrease in ATP in endothelial cells that was reflected in a reduction in eNOS-HSP90 interaction. Furthermore, this was associated with decreased NO and increased superoxide generation when the cells were exposed to fluid shear stress. This could be observed in vivo, where our data indicated that in the shunt lambs there was a progressive decrease in eNOS-HSP90 interactions. Furthermore, the decrease in eNOS-HSP90 interactions correlates with a progressive decrease in NO signaling and increases in NOS-derived superoxide. The progressive loss of NO signaling is a classic marker of endothelial dysfunction.

In conclusion, our data indicate that lambs with pulmonary hypertension secondary to increased pulmonary blood flow by 2 wk of age have developed mitochondrial dysfunction within the pulmonary system that is associated with progressive decreases in the interaction of eNOS with HSP90 and in NO generation. Furthermore, since our data indicate that this dysfunction is due to disruption of the carnitine homeostasis within the lung, the use of L-carnitine, or other carnitine analogs, may be of potential therapeutic benefit to help maintain eNOS-HSP90 interactions, NO signaling, and endothelial dysfunction.

GRANTS

This research was supported in part by National Heart, Lung, and Blood Institute Grants HL60190 (to S. M. Black), HL67841 (to S. M. Black),

HL72123 (to S. M. Black), HL70061 (to S. M. Black), and HL61284 (to J. R. Fineman) and by a grant from the Fondation LeDucq (to S. M. Black and J. R. Fineman).

REFERENCES

- Adnot S, Raffestin B, Eddahibi S, Braquet P, Chabrier PE. Loss of endothelium-dependent relaxant activity in the pulmonary circulation of rats exposed to chronic hypoxia. *J Clin Invest* 87: 155–162, 1991.
- Andrews ZB, Diano S, Horvath TL. Mitochondrial uncoupling proteins in the CNS: in support of function and survival. *Nat Rev* 6: 829–840, 2005.
- Beghetti M, Black SM, Fineman JR. Endothelin-1 in congenital heart disease. *Pediatr Res* 57: 16R–20R, 2005.
- Black SM, Fineman JR. Oxidative and nitrosative stress in pediatric pulmonary hypertension: roles of endothelin-1 and nitric oxide. *Vasc Pharmacol* 45: 308–316, 2006.
- Black SM, Fineman JR, Steinhorn RH, Bristow J, Soifer SJ. Increased endothelial NOS in lambs with increased pulmonary blood flow and pulmonary hypertension. *Am J Physiol Heart Circ Physiol* 275: H1643–H1651, 1998.
- Blomgren K, Zhu C, Hallin U, Hagberg H. Mitochondria and ischemic reperfusion damage in the adult and in the developing brain. *Biochem Biophys Res Commun* 304: 551–559, 2003.
- Bohles H, Evangelidou A, Bervoets K, Eckert I, Sewell A. Carnitine esters in metabolic disease. *Eur J Pediatr* 153: S57–S61, 1994.
- Bonawitz ND, Rodeheffer MS, Shadel GS. Defective mitochondrial gene expression results in reactive oxygen species-mediated inhibition of respiration and reduction of yeast life span. *Mol Cell Biol* 26: 4818–4829, 2006.
- Bonnefont JP, Djouadi F, Prip-Buus C, Gobin S, Munnich A, Bastin J. Carnitine palmitoyltransferases 1 and 2: biochemical, molecular and medical aspects. *Mol Aspects Med* 25: 495–520, 2004.
- Calvani M, Benatti P, Mancinelli A, D'Iddio S, Giordano V, Koverech A, Amato A, Brass EP. Carnitine replacement in end-stage renal disease and hemodialysis. *Ann NY Acad Sci* 1033: 52–66, 2004.
- Celermajer DS, Cullen S, Deanfield JE. Impairment of endothelium-dependent pulmonary artery relaxation in children with congenital heart disease and abnormal pulmonary hemodynamics. *Circulation* 87: 440–446, 1993.
- Chace DH, Pons R, Chiriboga CA, McMahon DJ, Tein I, Naylor EW, De Vivo DC. Neonatal blood carnitine concentrations: normative data by electrospray tandem mass spectrometry. *Pediatr Res* 53: 823–829, 2003.
- Chan PH. Mitochondrial dysfunction and oxidative stress as determinants of cell death/survival in stroke. *Ann NY Acad Sci* 1042: 203–209, 2005.
- DeVivo D, Tein I. Primary and secondary disorders of carnitine metabolism. *Int J Pediatr* 5: 135–141, 1990.
- Dewey CF Jr, Bussolari SR, Gimbrone MA Jr, Davies PF. The dynamic response of vascular endothelial cells to fluid shear stress. *J Biomech Eng* 103: 177–185, 1981.
- Duchen MR. Roles of mitochondria in health and disease. *Diabetes* 53, Suppl 1: S96–S102, 2004.
- Emerit J, Edeas M, Bricaire F. Neurodegenerative diseases and oxidative stress. *Biomed Pharmacother* 58: 39–46, 2004.
- Esposito L, Raber J, Kekonius L, Yan F, Yu GQ, Bien-Ly N, Puolivali J, Scearce-Levie K, Masliah E, Mucke L. Reduction in mitochondrial superoxide dismutase modulates Alzheimer's disease-like pathology and accelerates the onset of behavioral changes in human amyloid precursor protein transgenic mice. *J Neurosci* 26: 5167–5179, 2006.
- Fontana J, Fulton D, Chen Y, Fairchild TA, McCabe TJ, Fujita N, Tsuruo T, Sessa WC. Domain mapping studies reveal that the M domain of hsp90 serves as a molecular scaffold to regulate Akt-dependent phosphorylation of endothelial nitric oxide synthase and NO release. *Circ Res* 90: 866–873, 2002.
- Garcia-Cardena G, Fan R, Shah V, Sorrentino R, Cirino G, Papatropoulos A, Sessa WC. Dynamic activation of endothelial nitric oxide synthase by Hsp90. *Nature* 392: 821–824, 1998.
- Garvey EP, Oplinger JA, Tanoury GJ, Sherman PA, Fowler M, Marshall S, Harmon MF, Paith JE, Furfine ES. Potent and selective inhibition of human nitric oxide synthases. Inhibition by non-amino acid isothioureas. *J Biol Chem* 269: 26669–26676, 1994.
- Genova ML, Pich MM, Bernacchia A, Bianchi C, Biondi A, Bovina C, Falasca AI, Formiggini G, Castelli GP, Lenaz G. The mitochondrial production of reactive oxygen species in relation to aging and pathology. *Ann NY Acad Sci* 1011: 86–100, 2004.
- Giaid A, Saleh D. Reduced expression of endothelial nitric oxide synthase in the lungs of patients with pulmonary hypertension. *N Engl J Med* 333: 214–221, 1995.
- Gratton JP, Fontana J, O'Connor DS, Garcia-Cardena G, McCabe TJ, Sessa WC. Reconstitution of an endothelial nitric-oxide synthase (eNOS), hsp90, and caveolin-1 complex in vitro. Evidence that hsp90 facilitates calmodulin stimulated displacement of eNOS from caveolin-1. *J Biol Chem* 275: 22268–22272, 2000.
- Haworth JC, Demaugre F, Booth FA, Dilling LA, Moroz SP, Seshia SS, Seargeant LE, Coates PM. Atypical features of the hepatic form of carnitine palmitoyltransferase deficiency in a Hutterite family. *J Pediatr* 121: 553–557, 1992.
- Hinerfeld D, Traini MD, Weinberger RP, Cochran B, Doctrow SR, Harry J, Melov S. Endogenous mitochondrial oxidative stress: neurodegeneration, proteomic analysis, specific respiratory chain defects, and efficacious antioxidant therapy in superoxide dismutase 2 null mice. *J Neurochem* 88: 657–667, 2004.
- Hoffstedt J, Folkesson R, Wahrenberg H, Wennlund A, van Harmelen V, Arner P. A marked upregulation of uncoupling protein 2 gene expression in adipose tissue of hyperthyroid subjects. *Horm Metab Res* 32: 475–479, 2000.
- Iqbal M, Cawthon D, Wideman RF Jr, Bottje WG. Lung mitochondrial dysfunction in pulmonary hypertension syndrome. II. Oxidative stress and inability to improve function with repeated additions of adenosine diphosphate. *Poult Sci* 80: 656–665, 2001.
- Knowles PF, Gibson JF, Pick FM, Bray RC. Electron-spin-resonance evidence for enzymic reduction of oxygen to a free radical, the superoxide ion. *Biochem J* 111: 53–58, 1969.
- Konduri GG, Mattei J. Role of oxidative phosphorylation and ATP release in mediating birth-related pulmonary vasodilation in fetal lambs. *Am J Physiol Heart Circ Physiol* 283: H1600–H1608, 2002.
- Konduri GG, Mital S. Adenosine and ATP cause nitric oxide-dependent pulmonary vasodilation in fetal lambs. *Biol Neonate* 78: 220–229, 2000.
- Krauss S, Zhang CY, Lowell BB. A significant portion of mitochondrial proton leak in intact thymocytes depends on expression of UCP2. *Proc Natl Acad Sci USA* 99: 118–122, 2002.
- Krauss S, Zhang CY, Scorrano L, Dalgaard LT, St-Pierre J, Grey ST, Lowell BB. Superoxide-mediated activation of uncoupling protein 2 causes pancreatic beta cell dysfunction. *J Clin Invest* 112: 1831–1842, 2003.
- Kurtz DM, Tian L, Gower BA, Nagy TR, Pinkert CA, Wood PA. Transgenic studies of fatty acid oxidation gene expression in nonobese diabetic mice. *J Lipid Res* 41: 2063–2070, 2000.
- Liang LP, Patel M. Mitochondrial oxidative stress and increased seizure susceptibility in Sod2^{-/+} mice. *Free Radic Biol Med* 36: 542–554, 2004.
- Liu J, Atamna H, Kuratsune H, Ames BN. Delaying brain mitochondrial decay and aging with mitochondrial antioxidants and metabolites. *Ann NY Acad Sci* 959: 133–166, 2002.
- Liu J, Head E, Gharib AM, Yuan W, Ingersoll RT, Hagen TM, Cotman CW, Ames BN. Memory loss in old rats is associated with brain mitochondrial decay and RNA/DNA oxidation: partial reversal by feeding acetyl-L-carnitine and/or R-alpha-lipoic acid. *Proc Natl Acad Sci USA* 99: 2356–2361, 2002.
- Liu J, Killilea DW, Ames BN. Age-associated mitochondrial oxidative decay: improvement of carnitine acetyltransferase substrate-binding affinity and activity in brain by feeding old rats acetyl-L-carnitine and/or R-alpha-lipoic acid. *Proc Natl Acad Sci USA* 99: 1876–1881, 2002.
- Longo A, Bruno G, Curti S, Mancinelli A, Miotto G. Determination of L-carnitine, acetyl-L-carnitine and propionyl-L-carnitine in human plasma by high-performance liquid chromatography after pre-column derivatization with 1-aminoanthracene. *J Chromatogr B Biomed Appl* 686: 129–139, 1996.
- Marbach EP, Weil MH. Rapid enzymatic measurement of blood lactate and pyruvate. Use and significance of metaphosphoric acid as a common precipitant. *Clin Chem* 13: 314–325, 1967.
- Matsuishi T, Stumpf DA, Seliem M, Eguren LA, Chrislip K. Propionate mitochondrial toxicity in liver and skeletal muscle: acyl CoA levels. *Biochem Med Metab Biol* 45: 244–253, 1991.
- Mattson MP, Liu D. Mitochondrial potassium channels and uncoupling proteins in synaptic plasticity and neuronal cell death. *Biochem Biophys Res Commun* 304: 539–549, 2003.
- Minkler PE, Brass EP, Hiatt WR, Ingalls ST, Hoppel CL. Quantification of carnitine, acetylcarnitine, and total carnitine in tissues by high-

- performance liquid chromatography: the effect of exercise on carnitine homeostasis in man. *Anal Biochem* 231: 315–322, 1995.
44. **Misawa H, Nakata K, Matsuura J, Moriwaki Y, Kawashima K, Shimizu T, Shirasawa T, Takahashi R.** Conditional knockout of Mn superoxide dismutase in postnatal motor neurons reveals resistance to mitochondrial generated superoxide radicals. *Neurobiol Dis* 23: 169–177, 2006.
 45. **Moreira PI, Santos MS, Moreno AM, Proenca T, Seica R, Oliveira CR.** Effect of streptozotocin-induced diabetes on rat brain mitochondria. *J Neuroendocrinol* 16: 32–38, 2004.
 46. **Murray AJ, Anderson RE, Watson GC, Radda GK, Clarke K.** Uncoupling proteins in human heart. *Lancet* 364: 1786–1788, 2004.
 47. **Nishio Y, Kanazawa A, Nagai Y, Inagaki H, Kashiwagi A.** Regulation and role of the mitochondrial transcription factor in the diabetic rat heart. *Ann NY Acad Sci* 1011: 78–85, 2004.
 48. **Ohashi M, Runge MS, Faraci FM, Heistad DD.** MnSOD deficiency increases endothelial dysfunction in ApoE-deficient mice. *Arterioscler Thromb Vasc Biol* 26: 2331–2336, 2006.
 49. **Pande SV, Blanchaer MC.** Reversible inhibition of mitochondrial adenosine diphosphate phosphorylation by long chain acyl coenzyme A esters. *J Biol Chem* 246: 402–411, 1971.
 50. **Petersen KF, Dufour S, Befroy D, Garcia R, Shulman GI.** Impaired mitochondrial activity in the insulin-resistant offspring of patients with type 2 diabetes. *N Engl J Med* 350: 664–671, 2004.
 51. **Porter RK.** Mitochondrial proton leak: a role for uncoupling proteins 2 and 3? *Biochim Biophys Acta* 1504: 120–127, 2001.
 52. **Pritchard KA Jr, Ackerman AW, Gross ER, Stepp DW, Shi Y, Fontana JT, Baker JE, Sessa WC.** Heat shock protein 90 mediates the balance of nitric oxide and superoxide anion from endothelial nitric-oxide synthase. *J Biol Chem* 276: 17621–17624, 2001.
 53. **Reddy VM, Meyrick B, Wong J, Khor A, Liddicoat JR, Hanley FL, Fineman JR.** In utero placement of aortopulmonary shunts. A model of postnatal pulmonary hypertension with increased pulmonary blood flow in lambs. *Circulation* 92: 606–613, 1995.
 54. **Schulte TW, Akinaga S, Murakata T, Agatsuma T, Sugimoto S, Nakano H, Lee YS, Simen BB, Argon Y, Felts S, Toft DO, Neckers LM, Sharma SV.** Interaction of radicicol with members of the heat shock protein 90 family of molecular chaperones. *Mol Endocrinol* 13: 1435–1448, 1999.
 55. **Schulte TW, Akinaga S, Soga S, Sullivan W, Stensgard B, Toft D, Neckers LM.** Antibiotic radicicol binds to the N-terminal domain of Hsp90 and shares important biologic activities with geldanamycin. *Cell Stress Chaperones* 3: 100–108, 1998.
 56. **Shaul PW, Wells LB, Horning KM.** Acute and prolonged hypoxia attenuate endothelial nitric oxide production in rat pulmonary arteries by different mechanisms. *J Cardiovasc Pharmacol* 22: 819–827, 1993.
 57. **Shinde S, Glam K, Kumar P, Patil N, Sadacharan K.** Perioperative blood lactate levels, pyruvate levels, and lactate-pyruvate ratio in children undergoing cardiopulmonary bypass for congenital heart disease. *Indian J Crit Care Med* 9: 145–150, 2005.
 58. **Shug AL, Shrago E, Bittar N, Folts JD, Koke JR.** Acyl-CoA inhibition of adenine nucleotide translocation in ischemic myocardium. *Am J Physiol* 228: 689–692, 1975.
 59. **Sims NR, Anderson MF.** Mitochondrial contributions to tissue damage in stroke. *Neurochem Int* 40: 511–526, 2002.
 60. **Stanley CA.** New genetic defects in mitochondrial fatty acid oxidation and carnitine deficiency. *Adv Pediatr* 34: 59–88, 1987.
 61. **Stumpf DA, McAfee J, Parks JK, Eguren L.** Propionate inhibition of succinate:CoA ligase (GDP) and the citric acid cycle in mitochondria. *Pediatr Res* 14: 1127–1131, 1980.
 62. **Sullivan PG, Springer JE, Hall ED, Scheff SW.** Mitochondrial uncoupling as a therapeutic target following neuronal injury. *J Bioenerg Biomembr* 36: 353–356, 2004.
 63. **Szewczyk A, Wojtczak L.** Mitochondria as a pharmacological target. *Pharmacol Rev* 54: 101–127, 2002.
 64. **Vaz FM, Wanders RJ.** Carnitine biosynthesis in mammals. *Biochem J* 361: 417–429, 2002.
 65. **Vianey-Saban C, Mousson B, Bertrand C, Stamm D, Dumoulin R, Zabot MT, Divry P, Floret D, Mathieu M.** Carnitine palmitoyl transferase I deficiency presenting as a Reye-like syndrome without hypoglycaemia. *Eur J Pediatr* 152: 334–338, 1993.
 66. **Wainwright MS, Kohli R, Whittington PF, Chace DH.** Carnitine treatment inhibits increases in cerebral carnitine esters and glutamate detected by mass spectrometry after hypoxia-ischemia in newborn rats. *Stroke* 37: 524–530, 2006.
 67. **Wedgwood S, Bekker JM, Black SM.** Shear stress regulation of endothelial NOS in fetal pulmonary arterial endothelial cells involves PKC. *Am J Physiol Lung Cell Mol Physiol* 281: L490–L498, 2001.
 68. **Wedgwood S, Black SM.** Endothelin-1 decreases endothelial NOS expression and activity through ETA receptor-mediated generation of hydrogen peroxide. *Am J Physiol Lung Cell Mol Physiol* 288: L480–L487, 2005.
 69. **Wedgwood S, Mitchell CJ, Fineman JR, Black SM.** Developmental differences in the shear stress-induced expression of endothelial NO synthase: changing role of AP-1. *Am J Physiol Lung Cell Mol Physiol* 284: L650–L662, 2003.
 70. **Wiseman DA, Wells SM, Wilham J, Hubbard M, Welker JE, Black SM.** Endothelial response to stress from exogenous Zn²⁺ resembles that of NO-mediated nitrosative stress, and is protected by MT-1 overexpression. *Am J Physiol Cell Physiol* 291: C555–C568, 2006.
 71. **Woeltje KF, Kuwajima M, Foster DW, McGarry JD.** Characterization of the mitochondrial carnitine palmitoyltransferase enzyme system. II. Use of detergents and antibodies. *J Biol Chem* 262: 9822–9827, 1987.
 72. **Xue C, Johns RA.** Upregulation of nitric oxide synthase correlates temporally with onset of pulmonary vascular remodeling in the hypoxic rat. *Hypertension* 28: 743–753, 1996.